

Trajectories of directed lattice paths

EJ Janse van Rensburg^{2‡}

²Department of Mathematics and Statistics, York University, Toronto, Ontario M3J 1P3, Canada

E-mail: ‡rensburg@yorku.ca

31 January 2023

Abstract. The distribution of monomers along a linear polymer grafted on a hard wall is modelled by determining the probability distribution of occupied vertices of Dyck path and Dyck meander models of adsorbing linear polymers. For example, the probability that a Dyck path passes through the lattice site with coordinates $(\lfloor \epsilon n \rfloor, \lfloor \delta \sqrt{n} \rfloor)$ in the square lattice, for $0 < \epsilon < 1$ and $\delta \geq 0$, is determined asymptotically as $n \rightarrow \infty$ and this uncovers the probability density of vertices along Dyck paths in the limit as the length of the path n approaches infinity:

$$\mathbb{P}^{(D)}(\epsilon, \delta) = \frac{4\delta^2}{\sqrt{\pi} \epsilon^3 (1-\epsilon)^3} e^{-\delta^2/\epsilon(1-\epsilon)}.$$

The properties of a polymer coating of a hard wall and the density or distribution of monomers in the coating is relevant in applications such as the stabilisation of a colloid dispersion by a polymer or in a drug delivery system such as a drug-eluding stent covered by a grafted polymer.

Keywords: Directed lattice paths, directed polymers, density function, probability distribution, Dyck paths, adsorbed linear polymers

PACS numbers: 82.35.-x, 36.20.-r

AMS classification scheme numbers: 82B41, 82B23

1. Introduction

The physical properties of a polymer coating on surfaces or on suspended particles have been the subject of research for many decades. For example, linear polymers grafted on colloid particles or on other surfaces are important in biomedical and industrial applications including in the steric stabilisation of colloid dispersions [10, 21], or the use of polymers in drug delivery systems [18, 19, 24]. Examples of these drug delivery systems involve nanoparticle-polymer systems [25, 26], or polymer coatings on drug-eluding stents [9]. In these systems a polymer is adsorbed or grafted onto the surface (see figure 1 for a schematic diagram) and it coils from the surface to form a polymer layer in which the drug absorbs and is stabilised until it is delivered at a target site.

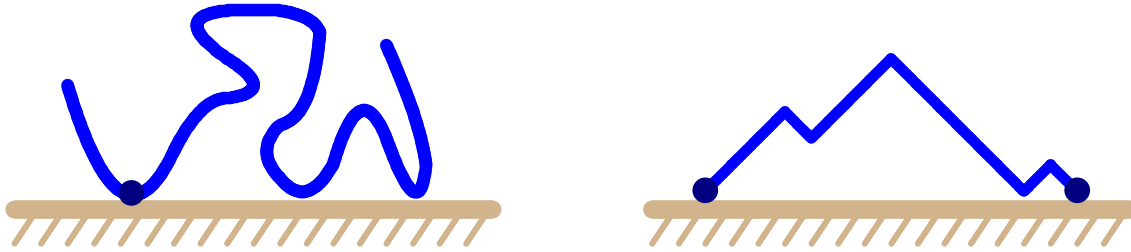


Figure 1: A schematic diagram of a linear polymer grafted on a surface (left). A Dyck path model of a grafted linear polymer (right). The Dyck path steps North-East or South-East in the square lattice, and it is grafted into the surface at its first and last nodes.

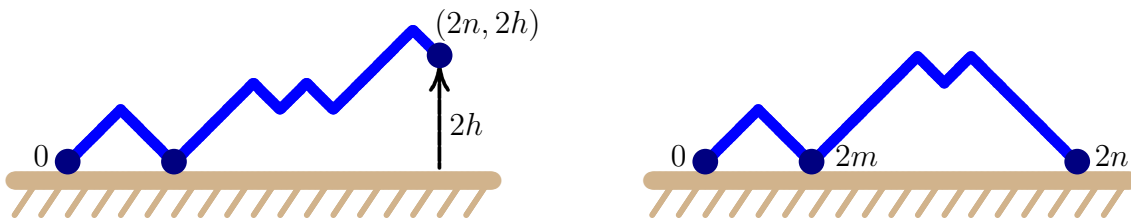


Figure 2: (Left) A Dyck meander from the origin to the point $(2n, 2h)$. The path steps in the half square lattice \mathbb{Z}_+^2 from the origin, has length $2n$ steps, and the height of its last node is $2h$. (Right) A Dyck path of length $2n$ from the origin, and passing through the vertex $(2m, 0)$.

The properties of the polymeric coating is of significant importance. If it is hydrophilic then it extends away from the surface forming a thicker and less dense coating. If, on the other hand, it is hydrophobic, then it forms a thinner and denser layer. Both these states may be important in applications, and from a physical perspective, the density profile of the polymeric coating may give indications of its suitability in an application.

In this paper the density profile of a grafted polymer is modelled using directed lattice paths. Directed models of adsorbing and grafted polymers were pioneered in references [8, 11, 12, 22, 28] and are useful in modelling entropic and scaling properties of linear polymers. The simplest of these models is shown in figure 1 and is a *Dyck path*. Dyck paths are directed lattice paths from the origin giving North-East and South-East steps in the upper half square lattice and are conditioned to end in the x -axis. The path visits the x -axis, and if these visits are weighed by a parameter a , then for large $a > 0$ the path adsorbs in the x -axis. This is a model of an adsorbing grafted linear polymer; see references [2, 3, 7, 14, 23]. Dyck path models of linear polymers are exactly solvable, and these models are still examined for both their mathematical properties, and as models of polymer entropy and phase behaviour [13, 15, 17].

The *half square lattice* is defined by $\mathbb{Z}_+^2 = \{(n, m) \mid n, m \in \mathbb{Z} \text{ and } m \geq 0\}$. The boundary of the half square lattice is $\partial\mathbb{Z}_+^2$ and it is also called the *hard wall* or *adsorbing wall*. A *directed path* from the origin in \mathbb{Z}_+^2 is a sequence of steps (edges) $(\langle u_i \sim u_{i+1} \rangle)$

such that $u_0 = (0, 0)$, $u_{i+1} = u_i + (1, \pm 1)$. If a vertex $u = (m, h)$ then h is the *height* of u . If the last vertex $u_n = (n, h)$, then the path has *length* n . That is, we consider a model of directed paths giving North-East or South-East steps in the half square lattice.

If a directed path in \mathbb{Z}_+^2 from the origin has length $2n$, and its last vertex has coordinates $u_{2n} = (2n, 0)$, then it is a *Dyck path* (and its last vertex has height zero).

A path from the origin and ending in a vertex at arbitrary height h is a *Dyck meander*. We shall abuse this terminology by simply calling them “meanders”.

A Dyck path is grafted at its first and last vertices in the hard wall or adsorbing wall, while a meander is grafted to the wall only at its first vertex. These models are illustrated in figure 2, and they are models of adsorbing grafted linear polymers.

The number of meanders of length $2n$ and ending in the vertex $(2n, 2h)$ is

$$D(2n, 2h) = \frac{2h+1}{n+h+1} \binom{2n}{n+h}. \quad (1)$$

Putting $h = 0$ gives the number of Dyck paths of length $2n$:

$$D(2n, 0) = \frac{1}{n+1} \binom{2n}{n}. \quad (2)$$

Note that $D(2n, 0) = C_n$ where the C_n are the Catalan numbers.

The vertices in a directed path are distributed in the area on and above the wall. For a given $n \in \mathbb{N}$, there is a probability that a directed path will pass through a vertex of coordinates $(2n, 2h)$. This is a (discrete) probability measure on the square lattice, which is zero outside the first quadrant and on vertices of odd parity (a vertex (n, m) has odd parity if $n + m$ is odd).

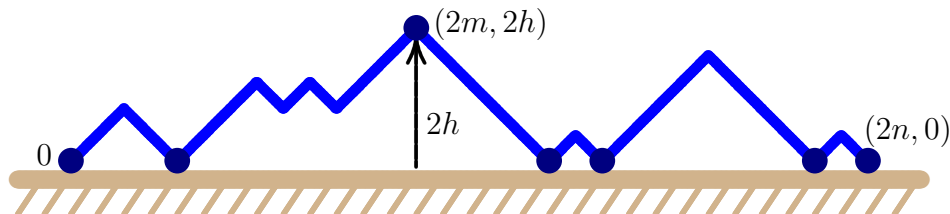


Figure 3: A Dyck path of length $2n$ passing through the vertex $(2m, 2h)$ is composed of two meanders (one reversed). The first meander is from the origin to the vertex $(2m, 2h)$, and the second starts in the vertex $(2n, 0)$ and then steps in the North-West and South-West directions until it terminates in $(2m, 2h)$.

The probability that a Dyck path of length $2n$ passes through the site with coordinates $(2m, 2h)$ (see figure 3) is given by the ratio of the number of Dyck paths passing through $(2m, 2h)$ divided by the number of Dyck paths of length $2n$:

$$P_{2n}^{(D)}(2m, 2h) = \frac{D(2m, 2h) \cdot D(2n - 2m, 2h)}{D(2n, 0)}. \quad (3)$$

It can be checked that $\sum_{h \geq 0} P_{2n}^{(D)}(2m, 2h) = 1$. The probability $P_{2n}^{(D)}(2m, 2h)$ is conditioned on all the paths having the same weight, and are therefore uniformly

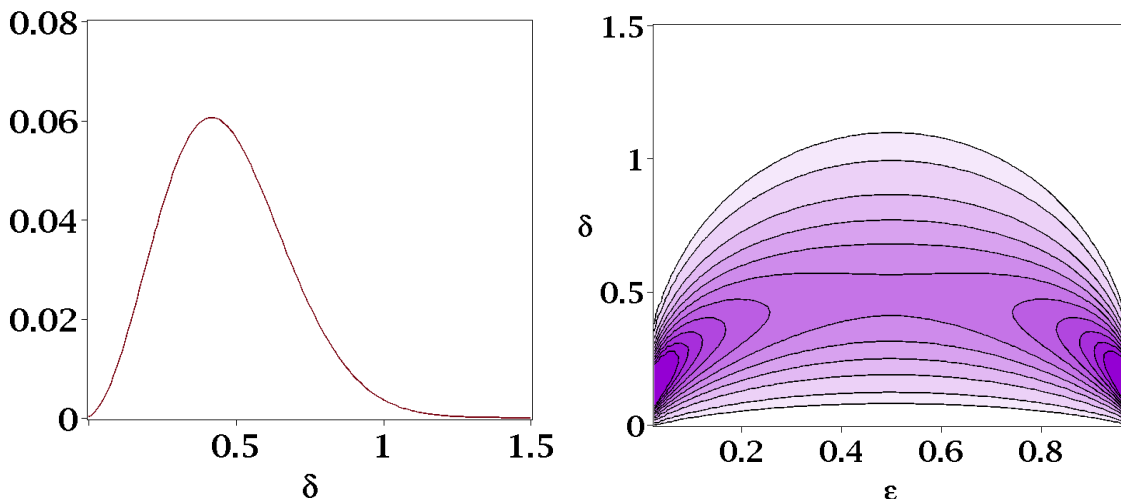


Figure 4: (Left) The probability that a Dyck path passes through a vertex of height $2\lfloor\delta\sqrt{n}\rfloor$ a fractional distance $\epsilon = 1/4$ along its total length $2n = 2000$. (Right) A contour plot of the probability density $P_{2n}^{(D)}(2\lfloor\epsilon n\rfloor, 2\lfloor\delta\sqrt{n}\rfloor)$ (equation (3)) for Dyck paths of total length $2n = 2000$.

sampled in this model. That is, $P_{2n}^{(D)}(2m, 2h)$ is the probability that a randomly sampled path passes through the point with coordinates $(2m, 2h)$. The natural scaling underlying this model is $O(n)$ in the horizontal direction and $O(\sqrt{n})$ in the vertical direction, since the directed path is a random walk in the vertical direction. Thus, introduce the scaling $m = \lfloor\epsilon n\rfloor$ and $h = \lfloor\delta\sqrt{n}\rfloor$ in equation (3). Plotting $P_{2n}^{(D)}(2\lfloor\epsilon n\rfloor, 2\lfloor\delta\sqrt{n}\rfloor)$ for $2n = 2000$ against δ for $\epsilon = 0.25$ gives the distribution in figure 4(left). This shows a peak well away from the hard wall, indicating that the path tends to drift away from the wall.

In the right panel of figure 4 a contour plot of $P_{2n}^{(D)}(2\lfloor\epsilon n\rfloor, 2\lfloor\delta\sqrt{n}\rfloor)$ for $2n = 2000$ is shown in the $\epsilon\delta$ -plane (with $0 < \epsilon < 1$ and $\delta > 0$). The parameter ϵ is the fractional distance along the x -axis, while δ is the rescaled height of vertices in the path (such that $\delta \approx h/\sqrt{n}$). This shows that in probability, the path drifts away from the hard wall, and only returns at its endpoint, visiting the hard wall infrequently.

Taking the limit $n \rightarrow \infty$ (with scaling $m = \lfloor\epsilon n\rfloor$ and $h = \lfloor\delta\sqrt{n}\rfloor$) gives the limiting probability density function

$$\mathbb{P}^{(D)}(\epsilon, \delta) = \lim_{n \rightarrow \infty} P_{2n}^{(D)}(2\lfloor\epsilon n\rfloor, 2\lfloor\delta\sqrt{n}\rfloor) = \frac{4\delta^2 e^{-\delta^2/\epsilon(1-\epsilon)}}{\sqrt{\pi \epsilon^3 (1-\epsilon)^3}}. \quad (4)$$

It can be checked that $\int_0^\infty \mathbb{P}^{(D)}(\epsilon, \delta) d\delta = \int_0^1 \int_0^\infty \mathbb{P}^{(D)}(\epsilon, \delta) d\delta d\epsilon = 1$. While equation (4) is exact, its derivation was not done with complete mathematical rigour. In this paper, our aim is to derive exact probability densities for the models of Dyck paths, rather than providing proofs that our results are exact.

The probability density in equation (4) induces a probability measure $d\rho(\epsilon, \delta)$ so that the probability of a path moving through a subset $A \subseteq \mathbb{R}^2$, in the scaling ($n = \infty$)

limit is given by

$$\mathbb{P}(A) = \int_A \mathbb{P}^{(D)}(\epsilon, \delta) d\lambda = \int_A \frac{d\rho(\epsilon, \delta)}{d\lambda} d\lambda = \int_A d\rho(\epsilon, \delta), \quad (5)$$

where λ is plane measure, and $\mathbb{P}^{(D)}(\epsilon, \delta)$ is the Radon-Nikodym derivative of $\rho(\epsilon, \delta)$ with respect to plane measure λ . The probability density $\mathbb{P}^{(D)}(\epsilon, \delta)$ is defined everywhere in \mathbb{R}^2 and is bigger than zero only when $(\epsilon, \delta) \in [0, 1] \times [0, \infty)$. In figure 5 a contour plot of $\mathbb{P}^{(D)}(\epsilon, \delta)$ is shown. Areas in a darker shade have higher probability densities.

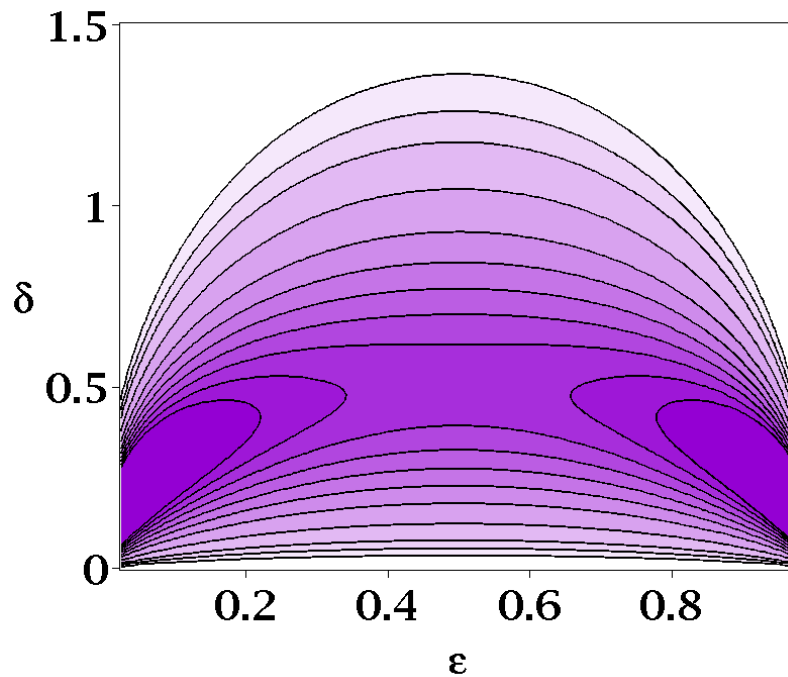


Figure 5: The probability density $\mathbb{P}^{(D)}(\epsilon, \delta)$ (equation (4)) of a Dyck path passing through points in the $\epsilon\delta$ -plane in the continuum limit.

The *mean path* can be calculated by integrating

$$\bar{\delta}(\epsilon) = \int_0^\infty \delta \mathbb{P}^{(D)}(\epsilon, \delta) d\delta = (2/\sqrt{\pi})\sqrt{\epsilon(1-\epsilon)}. \quad (6)$$

The *modal path* is obtained by determining that value of δ maximizing $\mathbb{P}^{(D)}(\epsilon, \delta)$. In this case it is given by

$$\delta_M(\epsilon) = \sqrt{\epsilon(1-\epsilon)}. \quad (7)$$

In general, the probability that the path stays underneath the curve $c(x) = x\sqrt{\epsilon(1-\epsilon)}$ is determined by noting that

$$p(x) = \int_0^1 \int_0^{c(x)} \mathbb{P}^{(D)}(\epsilon, \delta) d\delta d\epsilon = \text{erf}(x) - (2/\sqrt{\pi})e^{-x^2}. \quad (8)$$

Putting $x = 1$ gives the probability of staying underneath the modal curve, and this evaluates to $p(1) = 0.42759\dots$, while underneath the mean path $p(2/\sqrt{\pi}) = 0.53305\dots$

In contrast, $c(1/4) \approx 0.01132\dots$, and this is a low probability. Notice that $p(x) \simeq 4x^3/3\sqrt{3} + O(x^4)$ so that even for $x = 0.1$, $p(x)$ is very small. These results suggest that there is an area underneath the mean or modal path with a low probability of being occupied. This is consistent with the observations that a grafted polymer layer will absorb molecules as noted earlier in this introductory section, or that a grafted polymer experiences an entropic repulsion from the hard wall, swelling it away from the hard wall and creating a low density region next to the hard wall which is shielded by higher monomer densities along the modal or mean paths.

In the next sections this paper is organised as follows. In section 2.1 the results above, namely equation (4) and the results following from it, are shown. The model is generalised to Dyck meanders in section 2.2. The results are consistent with those seen for Dyck paths, but the lifted or free endpoint of the path do give more general probability densities.

In section 3 a Dyck path model of *adsorbing* linear polymers is examined. Adsorbing Dyck path models have long been studied as a model of the adsorption transition in linear polymers grafted to a hard wall [2,8,11,12,22,23,28]. In this model the paths pass from a desorbed phase through a transition into an adsorbed phase. In the desorbed phase the paths tend to drift away from the hard wall, while in the adsorbed phase it tends to stay close to the hard wall. The critical point separating these phases is a continuous phase transition, and scaling of the model depends on the phase. The probability density of adsorbed paths is examined in section 3.1) and it shows that in the scaling limit the path adheres to the adsorbing wall, not making any excursions into bulk. At the critical point (this is also called the *special point*) the scaling limit changes and trajectories of the path well away from the hard wall may be seen. This is shown in section 3.2. In the desorbed phase the probability density is identical to that of Dyck Paths shown in figure 5 and equation (4), as argued in section 3.3. The results are briefly reviewed in the discussion section 4.

2. Probability densities in models of directed paths

2.1. Dyck Paths

By equations (1), (2) and (3), the probability of a Dyck path of (even) length $2n$ passing through the lattice site with coordinates $(2m, 2h)$ is

$$P_{2n}^{(D)}(2m, 2h) = \frac{(2h+1)^2(2n+1)}{(m+h+1)(n-m+h+1)} \frac{\binom{2m}{m+h} \binom{2(n-m)}{n-m+h}}{\binom{2n}{n}}. \quad (9)$$

Proceed by putting $m = \lfloor \epsilon n \rfloor$ and $h = \lfloor \delta \sqrt{n} \rfloor$, and convert this expression into factorials. These are approximated asymptotically using the approximation derived in equation (65) in Appendix A:

$$n! = \sqrt{\pi(2n+1/3)} n^n e^{-n} (1 + O(1/n^2)). \quad (10)$$

The asymptotics of $D(2n, 0)$ (Catalan numbers) are well known [27], and given by

$$D(2n, 0) = \frac{1}{\sqrt{\pi n^3}} 4^n (1 + O(1/n)). \quad (11)$$

It remains to determine asymptotic expressions for $D(2\lfloor \sigma n \rfloor, 2\lfloor \delta \sqrt{n} \rfloor)$ where $\sigma = \epsilon$ or $\sigma = 1 - \epsilon$. Converting the binomial coefficient into its component factorials, and using the Stirling approximation in equation (9) gives, after taking logarithms, followed by expanding each term and simplifying (using Maple [20])

$$\begin{aligned} \log D(2\lfloor \sigma n \rfloor, 2\lfloor \delta \sqrt{n} \rfloor) &= (1 + 2\sigma n) \log 2 + \log \sqrt{\sigma/\pi} + \log(\delta/(\sigma^2 n)) - \delta^2/\sigma \\ &\quad + (1/(2\delta) - \delta/\sigma)/\sqrt{n} + O(1/n). \end{aligned}$$

Exponentiating the above, and simplifying, gives

$$D(2\lfloor \sigma n \rfloor, 2\lfloor \delta \sqrt{n} \rfloor) = \frac{2\delta 4^{\sigma n}}{\sqrt{\pi \sigma^3 n}} e^{-(2\delta^3 \sqrt{n} + 2\delta^2 - \sigma)/(2\delta \sigma \sqrt{n})} \times (1 + O(1/n)). \quad (12)$$

Combining these expressions for $D(2n, 0)$, $D(2\lfloor \epsilon n \rfloor, 2\lfloor \delta \sqrt{n} \rfloor)$ and $D(2\lfloor (1 - \epsilon)n \rfloor, 2\lfloor \delta \sqrt{n} \rfloor)$ approximates the probability:

$$P_{2n}^{(D)}(2\lfloor \epsilon n \rfloor, 2\lfloor \delta \sqrt{n} \rfloor) = \frac{4\delta^2}{\sqrt{\pi n \epsilon^3 (1 - \epsilon)^3}} e^{-(\delta^3 \sqrt{n} + \delta^2 - \epsilon(1 - \epsilon))/(\delta \epsilon (1 - \epsilon) \sqrt{n})} \times (1 + O(1/n)). \quad (13)$$

The function $P_{2n}^{(D)}(2\lfloor \epsilon n \rfloor, 2\lfloor \delta \sqrt{n} \rfloor)$ is the probability that the path passes through the point $(2\lfloor \epsilon n \rfloor, 2\lfloor \delta \sqrt{n} \rfloor)$. In order to determine the probability density in the limit as $n \rightarrow \infty$, notice that the area element $\Delta A = \Delta m \Delta h$ has scaling with n determined by $\Delta m = \lfloor \epsilon n \rfloor - \lfloor \epsilon(n-1) \rfloor \propto \epsilon$ and $\Delta h = \lfloor \delta \sqrt{n} \rfloor - \lfloor \delta \sqrt{n-1} \rfloor \propto \delta/\sqrt{n}$. That is, the area element ΔA scales proportional to $1/\sqrt{n}$. By multiplying equation (13) by \sqrt{n} and then taking $n \rightarrow \infty$, the probability density

$$\mathbb{P}^{(D)}(\epsilon, \delta) = \frac{4\delta^2 e^{-\delta^2/\epsilon(1-\epsilon)}}{\sqrt{\pi \epsilon^3 (1-\epsilon)^3}} \quad (14)$$

is obtained (see equation (4)). This density induces a probability measure $\rho(\epsilon, \delta)$ on \mathbb{R}^2 so that $d\rho(\epsilon, \delta) = \mathbb{P}^{(D)}(\epsilon, \delta) d\lambda$ where λ is plane measure. The properties of $\mathbb{P}^{(D)}(\epsilon, \delta)$ were already discussed in section 1.

An alternative (to the above) approach is to check the normalisation of equation (13). Integrating this equation over δ gives

$$\int_0^\infty P_{2n}^{(D)}(2\lfloor \epsilon n \rfloor, 2\lfloor \delta \sqrt{n} \rfloor) d\delta = 1/\sqrt{n} + O(1/n) \quad (15)$$

showing that the normalisation of equation (9) is lost when the substitutions $m = \lfloor \epsilon n \rfloor$ and $h = \lfloor \delta \sqrt{n} \rfloor$ are made, followed by an asymptotic expansion in n (and the limit $n \rightarrow \infty$ is taken). In particular, as pointed out above, this is due to the scaling of an area element when the summation is approximated by an integral. Thus, as $n \rightarrow \infty$, equation (13) must be multiplied by \sqrt{n} to recover the correct normalisation of the probability measure in equation (14).

2.2. Dyck meanders

Generalising to Dyck meanders gives the model in figure 6 which shows a meander ending in a vertex at height $2k$ having passed through the vertex with coordinates $(2m, 2h)$. The case with an endpoint fixed at height $2\lfloor\omega\sqrt{n}\rfloor$ is considered first, before the model with a free endpoint is examined. An approach similar to that of the last section is followed, but the extra degree of freedom in the model poses some additional challenges.

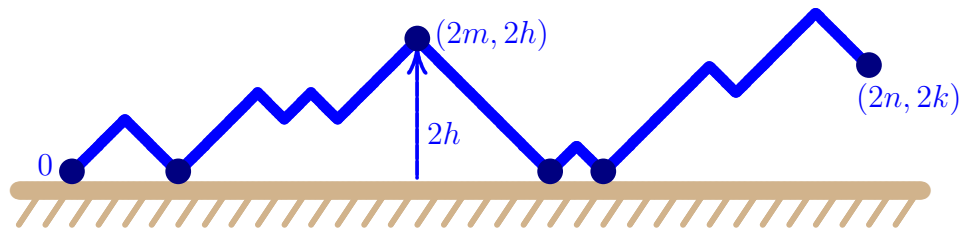


Figure 6: A meander of length $2n$ passing through the vertex $(2m, 2h)$. The path is partitioned at this vertex into a meander, and then a directed path from a vertex of height $2h$ to its endpoint at height $2k$.

The number of meanders of length $2n$ from the origin to the site $(2n, 2h)$ is given in equation (1), while the number of directed paths from a site at height $2h_0$ to a site at height $2h$, is given by

$$B(2n, 2h_0, 2h) = \binom{2n}{n+h-h_0} - \binom{2n}{n+h+h_0+1}. \quad (16)$$

The probability that a path from the origin passes through the site $(2m, 2h)$, conditioned to end in the site $(2n, 2k)$, is given by

$$P_{2n}^{(B)}(2m, 2h, 2k) = \frac{D(2m, 2h) \cdot B(2n-2m, 2h, 2k)}{D(2n, 2k)}. \quad (17)$$

Putting $m = \lfloor\epsilon n\rfloor$, $h = \lfloor\delta n\rfloor$, and $k = \lfloor\omega n\rfloor$, note that the asymptotics for $D(2\lfloor\epsilon n\rfloor, 2\lfloor\delta\sqrt{n}\rfloor)$ were already calculated in equation (12). This also gives by substitution an asymptotic formula for $D(2n, 2\lfloor\omega\sqrt{n}\rfloor)$. It remains to determine an asymptotic formula for $B(2n-2\lfloor\epsilon n\rfloor, 2\lfloor\delta\sqrt{n}\rfloor, 2\lfloor\omega\sqrt{n}\rfloor)$.

More generally, consider $B(2\lfloor\sigma n\rfloor, 2\lfloor\delta\sqrt{n}\rfloor, 2\lfloor\omega\sqrt{n}\rfloor)$ for $0 < \sigma \leq 1$, and $\delta > 0$ and $\omega > 0$ (where $\sigma = 1 - \epsilon$). Proceed by considering the first binomial coefficient in equation (16). Using Stirling's approximation to approximate the binomial coefficient, taking logarithms, simplifying and taking an asymptotic expansion, then exponentiating and simplifying gives (see equation (70) in Appendix A)

$$\binom{2\lfloor\sigma n\rfloor}{\lfloor\sigma n\rfloor + \lfloor\omega\sqrt{n}\rfloor - \lfloor\delta\sqrt{n}\rfloor} = \frac{e^{-(4(2\sigma n-1)(\delta-\omega)^2 + \sigma)/(8\sigma^2 n)}}{\sqrt{\pi\sigma n}} 4^{\sigma n} (1 + O(\sigma^{-2}n^{-2})). \quad (18)$$

Similarly, a slightly more complicated expression is obtained for the second binomial coefficient in equation (16):

$$\binom{2\lfloor\sigma n\rfloor}{\lfloor\sigma n\rfloor + \lfloor\omega\sqrt{n}\rfloor + \lfloor\delta\sqrt{n}\rfloor + 1}$$

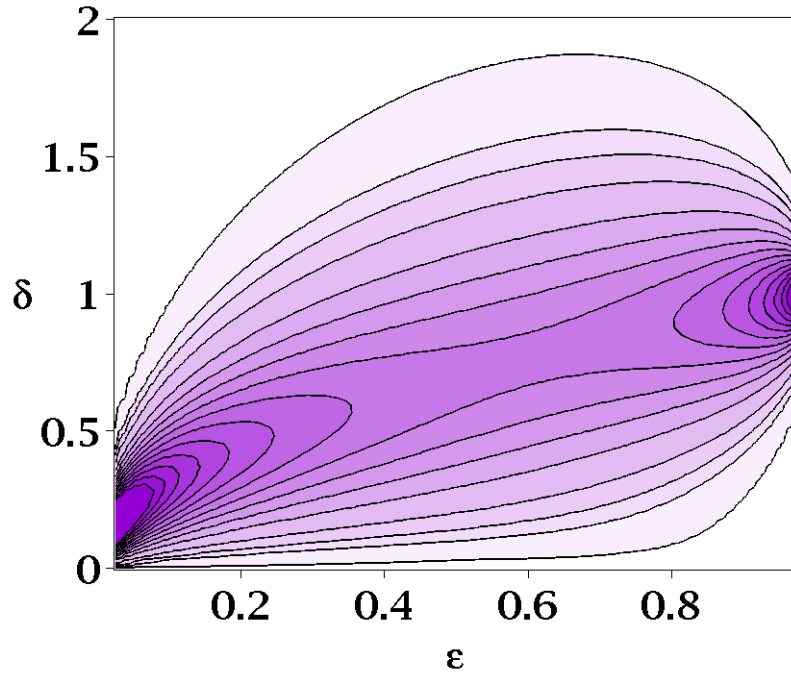


Figure 7: The probability density $\mathbb{P}^{(B)}(\epsilon, \delta, \omega)$ of a meander passing through points in the $\epsilon\delta$ -plane with $\omega = 1$.

$$= \frac{e^{-(4n(2\sigma n-1)(\delta+\omega)^2 + \sigma + 8(2\sigma n-1)(\delta+\omega)/\sqrt{n})/(8\sigma^2 n)}}{\sqrt{\pi\sigma n}} 4^{\sigma n} (1 + O(\sigma^{-2}n^{-2})). \quad (19)$$

Subtracting equation (19) from equation (18) will give the appropriate asymptotic approximation for $B(2\lfloor\sigma n\rfloor, 2\lfloor\alpha\sqrt{n}\rfloor, 2\lfloor\omega\sqrt{n}\rfloor)$.

Substituting the approximations in equations (18) and (19) in equation (17) and using equation (12) give an approximation to $P_{2n}(2\lfloor\epsilon n\rfloor, 2\lfloor\delta n\rfloor, 2\lfloor\omega n\rfloor)$. Simplifying and taking the asymptotic expansion for large n and keeping only the leading order term gives

$$P_{2n}^{(B)}(2\lfloor\epsilon n\rfloor, 2\lfloor\delta\sqrt{n}\rfloor, 2\lfloor\omega\sqrt{n}\rfloor) = \frac{\delta(1 - e^{-4\delta\omega/(1-\epsilon)})e^{-(\epsilon\omega-\delta)^2/\epsilon(1-\epsilon)}}{\omega\sqrt{\pi n\epsilon^3(1-\epsilon)}} (1 + O(1/\sqrt{n})). \quad (20)$$

Normalising again by multiplying with \sqrt{n} , and then taking $n \rightarrow \infty$, gives the probability density

$$\mathbb{P}^{(B)}(\epsilon, \delta, \omega) = \frac{\delta(1 - e^{-4\delta\omega/(1-\epsilon)})e^{-(\epsilon\omega-\delta)^2/\epsilon(1-\epsilon)}}{\omega\sqrt{\pi\epsilon^3(1-\epsilon)}}. \quad (21)$$

Integrating for $\delta > 0$ shows that this is normalised. A contourplot with $\omega = 1$ is shown in figure 7.

The mean path can be calculated and is given by

$$\begin{aligned} \bar{\delta}(\epsilon) &= \int_0^\infty \delta \mathbb{P}^{(B)}(\epsilon, \delta, \omega) d\delta \\ &= \frac{2\epsilon\omega^2 - \epsilon + 1}{2\omega} \operatorname{erf}\left(\omega\sqrt{\epsilon/(1-\epsilon)}\right) + \sqrt{\epsilon(1-\epsilon)}/\pi e^{-\epsilon\omega^2/(1-\epsilon)}. \end{aligned}$$

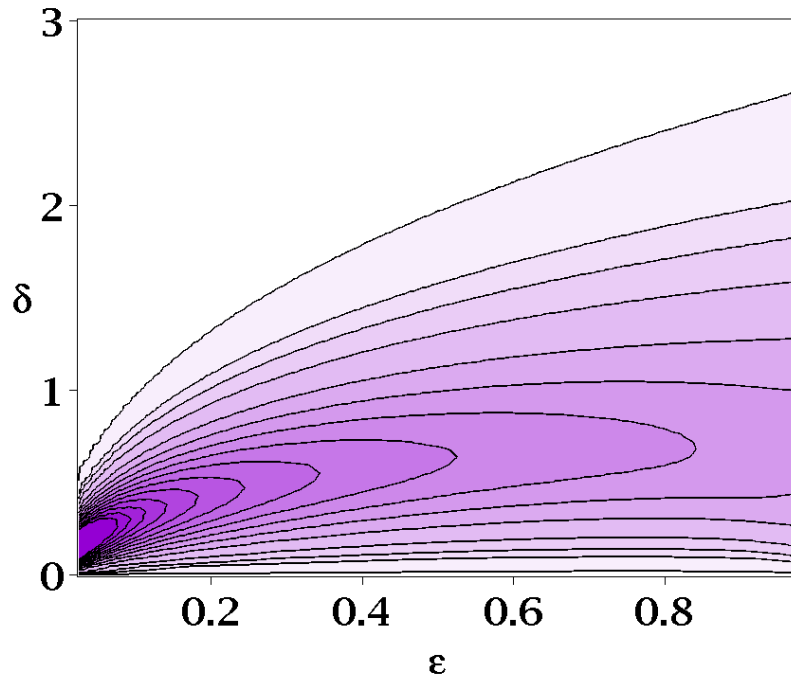


Figure 8: The probability density $\mathbb{P}^{(F)}(\epsilon, \delta, \omega)$ of a meander with a free endpoint passing through points in the $\epsilon\delta$ -plane.

The modal path is obtained by taking the derivative of equation (21) to obtain an implicit expression relating δ to ϵ :

$$e^{-4\delta\omega/(1-\epsilon)} (2\delta\epsilon\omega + 2\delta^2 + \epsilon^2 - \epsilon) + (2\delta\epsilon\omega - 2\delta^2 - \epsilon^2 + \epsilon) = 0. \quad (22)$$

This can be simplified to

$$\tanh\left(\frac{2\delta\omega}{1-\epsilon}\right) = \frac{2\delta\epsilon\omega}{2\delta^2 + \epsilon^2 - \epsilon}. \quad (23)$$

If ω is small, then the approximation $\tanh x \approx x - x^3/3$ can be used to obtain, after an expansion in ω , followed by exponentiation,

$$\delta_M(\epsilon) \approx \sqrt{\epsilon(1-\epsilon)} e^{\epsilon\omega^2/3(1-\epsilon)}. \quad (24)$$

This approximation is accurate for small ϵ , but breaks down as $\epsilon \rightarrow 1^-$. For large ω approximate $\tanh(x) \approx 1$ to obtain

$$\delta_M(\epsilon) \approx \frac{1}{2} \left(\epsilon\omega + \sqrt{(\omega^2 - 2)\epsilon^2 + 2\epsilon} \right). \quad (25)$$

This approximation is in particular accurate for ϵ approaching 1.

The density function can also be obtained for a model with a free endpoint. Subtracting equation (19) from equation (18) gives an approximation for $B([\sigma n], [\delta\sqrt{n}], [\omega\sqrt{n}])$ with the same leading error terms as in Appendix A equation (70) where $\lambda = \sigma$, $\delta = \delta$ and $\kappa = \omega$. Since the error terms are constant, or decay to zero as $\omega \rightarrow \infty$, $B([\sigma n], [\delta\sqrt{n}], [\omega\sqrt{n}])$ can be integrated over $\omega \in (0, \infty)$ for fixed $\delta > 0$ to

obtain an asymptotic approximation for the number of paths of length $\lfloor \sigma n \rfloor$ starting at height $\lfloor \delta \sqrt{n} \rfloor$.

Proceed by first integrating the right hand side of equation (18) for $\omega \in (0, \infty)$.

This gives

$$\frac{4^{\sigma n} \sqrt{\sigma} e^{-1/8\sigma n}}{\sqrt{4n\sigma - 2}} \left(1 + \operatorname{erf} \left(\frac{\delta \sqrt{2n\sigma - 1}}{\sqrt{2n}\sigma} \right) \right) = \frac{4^{\sigma n}}{\sqrt{4n}} \left(1 + \operatorname{erf} \left(\frac{\delta}{\sqrt{\sigma}} \right) + O(1/\sqrt{n^3}) \right).$$

Treating the right hand side of equation (19) the same way produces

$$\begin{aligned} \frac{4^{\sigma n} \sqrt{\sigma} e^{(\tau\sigma n - 4)/8\sigma^2 n^2}}{\sqrt{4n\sigma - 2}} & \left(1 - \operatorname{erf} \left(\frac{2\sigma \sqrt{n} + 2\sigma - 8/\sqrt{n} - 1/n}{\sigma \sqrt{4n\sigma - 2}} \right) \right) \\ & = \frac{4^{\sigma n}}{\sqrt{4n}} \left(1 - \operatorname{erf} \left(\frac{\delta}{\sqrt{\sigma}} \right) - \frac{2e^{-\delta^2/\sigma}}{\sqrt{\pi\lambda n}} + O(1/\sqrt{n^3}) \right). \end{aligned}$$

Subtract the last equation from the penultimate to obtain

$$\begin{aligned} F(\lfloor \sigma n \rfloor, \lfloor \delta \sqrt{n} \rfloor) & = \int_0^\infty B(\lfloor \sigma n \rfloor, \lfloor \delta \sqrt{n} \rfloor, \lfloor \omega \sqrt{n} \rfloor) d\omega \\ & = \frac{4^{\sigma n}}{\sqrt{n}} \left(\operatorname{erf}(\delta/\sqrt{\sigma}) + \frac{e^{-\delta^2/\sigma}}{\sqrt{\pi\lambda n}} + O(1/n) \right). \end{aligned} \quad (26)$$

The probability of a meander of length $2n$ from the origin, with a free endpoint, passing through the point $(2m, 2h)$ is

$$P_{2n}^{(F)}(2m, 2h) = \frac{D(2m, 2h) \cdot F(2(n-m), 2h)}{F(2n, 0)}. \quad (27)$$

Substituting $m = \lfloor \epsilon n \rfloor$ and $h = \lfloor \delta \sqrt{n} \rfloor$, and then using equations (12) and (26) gives

$$P_{2n}^{(F)}(2\lfloor \epsilon n \rfloor, 2\lfloor \delta \sqrt{n} \rfloor) = \frac{2\delta e^{-\delta^2/\epsilon}}{\sqrt{\epsilon^3}} \operatorname{erf}(\delta/\sqrt{1-\epsilon}) + O(1/\sqrt{n}). \quad (28)$$

Taking $n \rightarrow \infty$ gives the probability density (see figure 8)

$$\mathbb{P}^{(F)}(\epsilon, \delta) = \frac{2\delta e^{-\delta^2/\epsilon}}{\sqrt{\epsilon^3}} \operatorname{erf}(\delta/\sqrt{1-\epsilon}). \quad (29)$$

The normalisation of this probability density is also sound, since

$$\int_0^\infty \mathbb{P}^{(F)}(\epsilon, \delta) d\delta = 1. \quad (30)$$

The modal path is given by the solution $\delta_M(\epsilon)$ of

$$\operatorname{erf} \left(\frac{\delta}{\sqrt{1-\epsilon}} \right) = \frac{2\delta\epsilon e^{-\delta^2/(1-\epsilon)}}{(2\delta^2 - \epsilon)\sqrt{\pi(1-\epsilon)}}. \quad (31)$$

In the case that δ and ϵ are small, the modal path can be approximated by

$$\delta_M(\epsilon) \approx \sqrt{\frac{3\epsilon}{2\epsilon + 3}} = \sqrt{\epsilon} - \sqrt{\epsilon^3}/3 + \sqrt{\epsilon^5}/6 - \dots. \quad (32)$$

In the event that $\epsilon \rightarrow 1^-$, the path approaches $\delta(1) = 1/\sqrt{2}$. To see this, write equation (31) in the following form

$$\frac{e^{-\delta^2/(1-\epsilon)}}{\sqrt{\pi(1-\epsilon)} \operatorname{erf}(\delta/\sqrt{1-\epsilon})} = \frac{2\delta^2 - \epsilon}{2\delta\epsilon}. \quad (33)$$

Take the left limit as $\epsilon \rightarrow 1^-$ shows that the left hand side approaches zero, so that one must have $2\delta^2 - 1 = 0$ showing that $\delta_M(1^-) = 1/\sqrt{2}$.

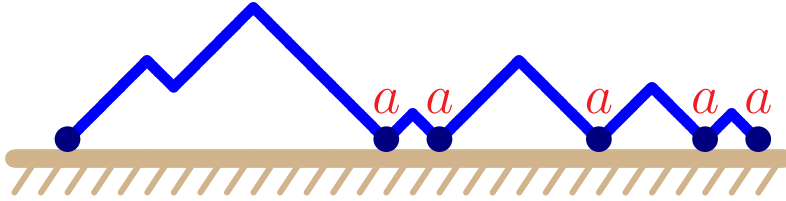


Figure 9: A Dyck path model of an adsorbing linear polymer grafted on a surface. Each return (visit) of the Dyck path the hard wall is weighted by an activity a . If a is large then conformations of the path with a large number of visits dominate the partition function, and the path is in an adsorbed state.

3. Adsorbing Dyck paths

Adsorbing Dyck paths (see figure 9) is a model of an adsorbing linear polymer [3–6, 23] with monomers which may stick to the adsorbing surface. The generating function of adsorbing Dyck paths is given by

$$D(a, t) = \frac{2}{2 - a(1 - \sqrt{1 - 4t^2})}, \quad (34)$$

where t is the generating variable for steps in the path, and a is the generating variable of returns (visits) of the path to the adsorbing (hard) wall. In order to analyse this model, consider directed paths of length $2n$ from a site $(0, 2h_0)$ to a site $(2n, 2h)$ as shown in figure 10. The partition function is given by (see equation (5.33) in reference [16])

$$d_n(h_0, h) = \binom{2n}{n+h-h_0} - \binom{2n}{n+h+h_0} + a \sum_{\ell=0}^{n-h-h_0} \left(\binom{2n}{n+h+h_0+\ell} - \binom{2n}{n+h+h_0+\ell+1} \right) (a-1)^\ell. \quad (35)$$

The difference between the first two binomial coefficients counts paths having no intersection with the adsorbing wall, while the summation over ℓ counts paths intersecting the adsorbing wall at least once.

The generating function in equation (34) shows a critical adsorption point at the critical activity $a_c = 2$, and this is the *special point*. For $a > 2$ the model is in an adsorbed state, with paths intersecting the adsorbing wall dominating the partition function. If $a < 2$, then the first two binomial coefficients dominate equation (35), and the path is desorbed.

3.1. The density of adsorbed directed paths (for $a > 2$)

Since we will ultimately only be interested in paths starting at the origin (so that $h_0 = 0$), the first two binomial coefficients can be ignored in equation (35).

Put $A = a - 1$ and denote the summand in equation (35) by

$$S(\ell) = \frac{1}{n+h_0+h+\ell+1} \binom{2n}{n+h_0+h+\ell} A^\ell. \quad (36)$$

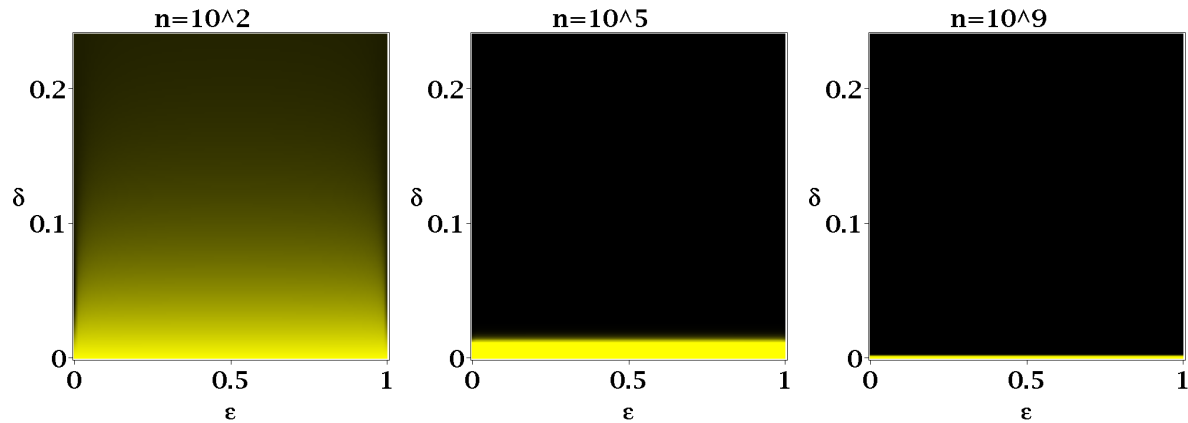


Figure 11: The probability $P_{2n}^{(C)}(2[\epsilon n], 2[\delta])$ of an adsorbing Dyck path with activity $a = 3$.

Calculating $\lambda F(\tau_s)$ and using the saddle point approximation then gives the following approximation of equation (35) when $m^2 = n$ (notice that the original substitution was $n = \lfloor \sigma m^2 \rfloor$) and $h + h_0 = \alpha\sqrt{n}$:

$$f(\sigma, \alpha) = \left(\frac{(A+1)^2}{A} \right)^{\sigma n + 1/2} \frac{e^{-\alpha^2(A+1)^2/\sigma A}}{2\sigma n^2 A^{\alpha\sqrt{n} + 1/2}}. \quad (42)$$

The function $f(\sigma, \alpha)$ is a finite size approximation to the partition function of directed paths of length $\lfloor 2\sigma n \rfloor$, adsorbing into a hard wall, and with the combined height of its endpoints $h_0 + h = \lfloor \alpha\sqrt{n} \rfloor$.

The probability that the path passes through the point $(2[\epsilon n], 2[\delta\sqrt{n}])$ having started in the origin, and then ending in the adsorbing wall, is

$$\begin{aligned} P_{2n}^{(C)}(2[\epsilon n], 2[\delta\sqrt{n}]) &\approx \frac{f(\epsilon, \delta) \cdot f(1-\epsilon, \delta)}{f(1, 0)} \\ &= \left(\frac{(A+1)}{2n^2 \epsilon(1-\epsilon)} \right) A^{-2\delta\sqrt{n}-1} e^{-\delta^2(A+1)^2/4\epsilon(1-\epsilon)A}. \end{aligned} \quad (43)$$

Due to the approximations used to derive this expression, it is not normalised, and must be, so integrate $\delta \in [0, \infty)$. This produces an expression containing error functions, which is again expanded asymptotically. Substituting and then simplifying gives the final approximation of the finite size probability:

$$P_{2n}^{(C)}(2[\epsilon n], 2[\delta\sqrt{n}]) \simeq 2\sqrt{n} (\log A) A^{-2\delta\sqrt{n}} e^{-\delta^2(A+1)^2/4\epsilon(1-\epsilon)A}. \quad (44)$$

As expected, this result breaks down when $a = 2$ (or $A = 1$). In figure 11 three density plots are shown for $n = 10^2$, $n = 10^5$ and $n = 10^9$. Notice the narrow (vertical) range of δ . The density concentrates towards $\delta = 0$ with increasing n , from a more diffused density when $n = 10^2$, to a very narrow bar along $\delta = 0$ when $n = 10^9$. These plots are for $a = 3$.

Consider next a closed rectangle $R = [\epsilon_1, \epsilon_2] \times [\delta_1, \delta_2]$ with $0 \leq \epsilon_1 < \epsilon_2 \leq 1$ and $0 < \delta_1 < \delta_2 < \infty$. The probability that the path passes through R is given by

$$\text{Prob}_n(R) = \int_R P_{2n}^{(C)}(2\lfloor \epsilon n \rfloor, 2\lfloor \delta \sqrt{n} \rfloor) d\lambda + [\text{finite size corrections}], \quad (45)$$

up to finite size corrections which decay as n approaches infinity, and where λ is plane measure. Since $\delta_1 > 0$, it follows that

$$\begin{aligned} \lim_{n \rightarrow \infty} \text{Prob}_n(R) &= \lim_{n \rightarrow \infty} \int_R P_{2n}^{(C)}(2\lfloor \epsilon n \rfloor, 2\lfloor \delta \sqrt{n} \rfloor) d\lambda \\ &\leq \lim_{n \rightarrow \infty} P_{2n}^{(C)}(2\lfloor \delta_1 \sqrt{n} \rfloor, 0) \times \text{Area}(R) = 0. \end{aligned} \quad (46)$$

This result is true even in the limit that $\delta_2 \rightarrow \infty$. In other words, the probability that the path passes through the infinite rectangle $[\epsilon_1, \epsilon_2] \times [\delta_1, \infty)$ is zero, for any $\delta_1 > 0$, and for $0 \leq \epsilon_1 < \epsilon_2 \leq 1$.

If $\delta_1 = 0$, then consider the rectangle $R = [\epsilon_1, \epsilon_2] \times [0, \delta_2)$. Define the infinite rectangle $R_\infty = [\epsilon_1, \epsilon_2] \times [0, \infty)$ and put $R_2 = [\epsilon_1, \epsilon_2] \times [\delta_2, \infty) = R_\infty \setminus R$. Then it follows that

$$\lim_{n \rightarrow \infty} \text{Prob}_n(R_\infty) = \epsilon_2 - \epsilon_1 \quad (47)$$

since $P_{2n}^{(C)}(2\lfloor \epsilon n \rfloor, 2\lfloor \delta \sqrt{n} \rfloor)$ in equation (44) is normalised in the $n \rightarrow \infty$ limit. However, by equation (46), since $R_\infty = R \cup R_2$ and $R \cap R_2 = \emptyset$,

$$\lim_{n \rightarrow \infty} \text{Prob}_n(R) = \lim_{n \rightarrow \infty} \text{Prob}_n(R_\infty) - \lim_{n \rightarrow \infty} \text{Prob}_n(R_2) = \lim_{n \rightarrow \infty} \text{Prob}_n(R_\infty) = \epsilon_2 - \epsilon_1. \quad (48)$$

Since this result is independent of $\delta_2 > 0$, take the limit $\delta_2 \rightarrow 0^+$, and define the set function $\xi(R)$ on rectangles R as follows: If $R = [\epsilon_1, \epsilon_2] \times [c_1, c_2]$, then

$$\xi(R) = \lim_{n \rightarrow \infty} \text{Prob}_n(R) = \begin{cases} 0, & \text{if } 0 \leq \epsilon_1 < \epsilon_2 \leq 1 \text{ and } 0 < c_1 < c_2; \\ \epsilon_2 - \epsilon_1, & \text{if } 0 \leq \epsilon_1 < \epsilon_2 \leq 1 \text{ and } 0 = c_1 < c_2; \\ 0, & \text{otherwise.} \end{cases} \quad (49)$$

Then ξ is a set-function on rectangles in the plane \mathbb{R}^2 and an outer measure ξ on sets $E \subseteq \mathbb{R}^2$ can be defined by

$$\xi E = \inf \left\{ \sum_j \xi R_j \mid E \subseteq \cup R_j \text{ and } \{R_j\} \text{ is a countable cover of } E \right\}, \quad (50)$$

where the infimum is taken over all countable covers of E by rectangles. Since $\xi \mathbb{R}^2 = 1$, ξ induces a probability measure $\mathbb{P}^{(C)}$ on the σ -algebra of plane measure sets, such that the limiting probability that a path passes through points in E is given by

$$\mathbb{P}^{(C)}(E) = \int_E d\xi = \int_E \frac{d\xi}{d\lambda} d\lambda = \int_E \mathbb{P}^{(C)}(\epsilon, \delta) d\lambda \quad (51)$$

so that $d\xi = \mathbb{P}^{(C)}(\epsilon, \delta) d\lambda$ and $\mathbb{P}^{(C)}(\epsilon, \delta)$ is the Radon-Nikodym derivative of ξ with respect to plane measure λ (and is the probability density of the model in the limit $n \rightarrow \infty$). Notice that $\mathbb{P}^{(C)}(\epsilon, \delta) = 0$ everywhere in the $\epsilon\delta$ -plane except on the line

segment $\delta = 0$ and $\epsilon \in [0, 1]$ but that it is normalised such that for $\delta > 0$, if $R_\delta = [0, 1] \times [0, \delta]$,

$$\begin{aligned} \int_{R_\delta} \mathbb{P}^{(C)}(\epsilon, \delta) d\lambda &= \lim_{\delta \rightarrow 0^+} \int_{R_\delta} \mathbb{P}^{(C)}(\epsilon, \delta) d\lambda \\ &= \int_0^1 \int_0^\infty \mathbb{P}^{(C)}(\epsilon, \delta) d\delta d\epsilon = \int_{\mathbb{R}^2} \mathbb{P}^{(C)}(\epsilon, \delta) d\lambda = 1. \end{aligned} \quad (52)$$

3.2. Paths at the special point

At the critical (special) point $a = 2$ equation (35) telescopes to

$$d_n(h_0, h) \Big|_{a=2} = \binom{2n}{n+h-h_0} + \binom{2n}{n+h+h_0} - 4n. \quad (53)$$

Substitute $n = \lfloor \sigma m^2 \rfloor$, $h_0 = \lfloor \alpha \sqrt{n} \rfloor$ and $h = \lfloor \omega \sqrt{n} \rfloor$. In order to determine the asymptotic behaviour at $a = 2$, consider the binomial terms above independently. As before, use equation (10) to approximate factorials, take logarithms, simplify and expand the resulting expressions asymptotically. Exponentiation the result gives

$$\binom{2\lfloor \sigma m^2 \rfloor}{\lfloor \sigma m^2 \rfloor + \lfloor \omega m \rfloor - \lfloor \alpha m \rfloor} \simeq \frac{4^{\sigma m^2}}{\sqrt{\pi \sigma} m} e^{-(\alpha-\omega)^2(6m\sigma^2-3\sigma+(\alpha-\omega)^2)/6\sigma^3 m^2}. \quad (54)$$

Similarly,

$$\binom{2\lfloor \sigma m^2 \rfloor}{\lfloor \sigma m^2 \rfloor + \lfloor \omega m \rfloor + \lfloor \alpha m \rfloor} \simeq \frac{4^{\sigma m^2}}{\sqrt{\pi \sigma} m} e^{-(\alpha+\omega)^2(6m\sigma^2-3\sigma+(\alpha+\omega)^2)/6\sigma^3 m^2}. \quad (55)$$

Combining these expressions, simplifying, taking logarithms, expanding asymptotically in m , replacing $m^2 = n$, and then exponentiating gives to leading order

$$\frac{4^{\sigma n} e^{-(\alpha^2+\omega^2)/\sigma}}{\sqrt{\pi \sigma n}} (e^{2\alpha\omega/\sigma} + e^{-2\alpha\omega/\sigma}) - 4\sigma n = \frac{4^{\sigma n+1/2} e^{-(\alpha^2+\omega^2)/\sigma}}{\sqrt{\pi \sigma n}} \cosh(2\alpha\omega/\sigma) - 4\sigma n. \quad (56)$$

The last term $4\sigma n$ can be ignored in the asymptotic limit. Thus, put

$$f(\sigma, \alpha, \omega) = \frac{4^{\sigma n+1/2} e^{-(\alpha^2+\omega^2)/\sigma}}{\sqrt{\pi \sigma n}} \cosh(2\alpha\omega/\sigma). \quad (57)$$

Using the same arguments as in section 2.2, the probability that the path passes through the point $(2\lfloor \epsilon n \rfloor, 2\lfloor \delta \sqrt{n} \rfloor)$ is asymptotically approximated by

$$P_{2n}^{(S)}(2\lfloor \epsilon n \rfloor, 2\lfloor \delta \sqrt{n} \rfloor) = \frac{2 e^{-\delta^2/\epsilon(1-\epsilon)}}{\sqrt{\pi \epsilon(1-\epsilon)}}. \quad (58)$$

Notice that all n -dependence has dropped out to leading order, so that this is also the probability density of the model. That is, taking $n \rightarrow \infty$ gives the density

$$\mathbb{P}^{(S)}(\epsilon, \delta) = \frac{2 e^{-\delta^2/\epsilon(1-\epsilon)}}{\sqrt{\pi \epsilon(1-\epsilon)}}. \quad (59)$$

The mean path is given by

$$\bar{\delta}(\epsilon) = \int_0^\infty \delta \mathbb{P}^{(S)}(\epsilon, \delta) d\delta = \sqrt{\epsilon(1-\epsilon)/\pi}. \quad (60)$$

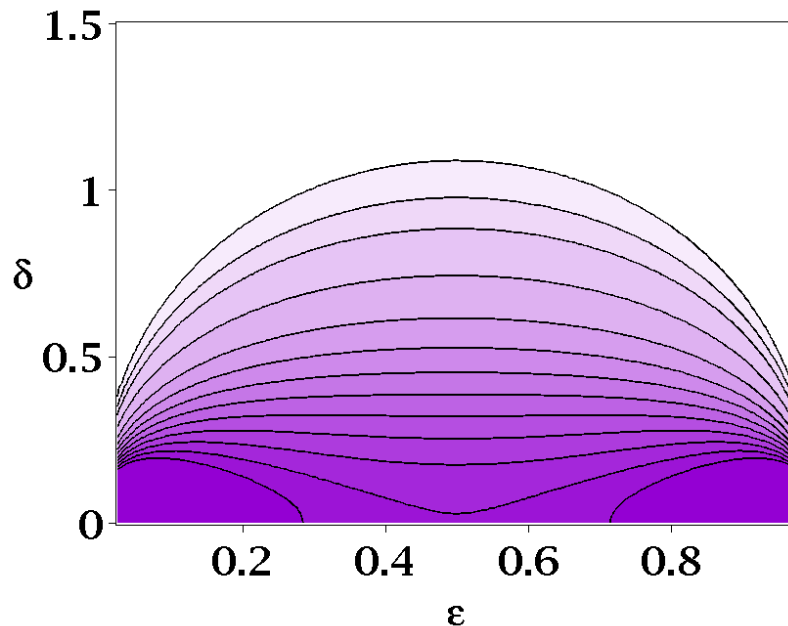


Figure 12: The probability density $\mathbb{P}^{(S)}(\epsilon, \delta)$ of an adsorbing Dyck path at the special point.

The modal path is obtained by solving $\frac{d}{d\delta} \log \rho(\epsilon, \delta) = 2\delta/\epsilon(1-\epsilon) = 0$. This shows

$$\delta_M(\epsilon) = 0, \quad \text{for } \epsilon \in [0, 1]. \quad (61)$$

This is expected, since at the critical point the path is adsorbed on the wall. The median path is obtained by solving for $\delta_m(\epsilon)$ in

$$\int_0^{\delta_m} \mathbb{P}^{(S)}(\epsilon, \delta) d\delta = \text{erf}\left(\delta_m/\sqrt{\epsilon(1-\epsilon)}\right) = 1/2. \quad (62)$$

A numerical solution gives

$$\delta_m(\epsilon) = z_0 \sqrt{\epsilon(1-\epsilon)} \approx 0.4769 \sqrt{\epsilon(1-\epsilon)} \quad (63)$$

where z_0 is the real solution of $2 \text{erf}(z) = 1$.

3.3. The case that $a < 2$.

In the event that $a < 2$ the saddle point τ_2 in equation (40) moves to a negative value. This shows, asymptotically, that $\tau = 0$ maximizes equation (37), and therefore that the $\ell = 0$ term in equation (36) is dominant in the asymptotic regime. Thus, putting $h_0 = 0$ in equation (35), gives the approximation

$$\begin{aligned} D(2n, 2h) = d_{2n}(0, 2h) &\lesssim a \sum_{\ell=0}^{\infty} \frac{1}{n+h+\ell+1} \binom{2n}{n+h+\ell} A^\ell \\ &\lesssim \frac{a}{2-a} \frac{1}{n+h+1} \binom{2n}{n+h}, \end{aligned}$$

since $A = a - 1$. Comparison to equation (1) and then using equation (3) gives expressions similar to equation (9) for the probability $P_{2n}^{(D)}(2m, 2h)$ passing through the point $(2m, 2h)$. Determining the asymptotics of this gives equation (14).

4. Discussion

In this paper the probability distributions of directed and adsorbing directed paths were determined. The results are exact, but were not proven with full mathematical rigour (that will require the tracking of error terms in the asymptotic approximations). We collect our results in table 1 below.

Table 1: Probability densities of adsorbing directed paths

Model	$\mathbb{P}(\epsilon, \delta, \dots)$
Dyck paths	$\frac{4\delta^2}{\sqrt{\pi \epsilon^3 (1-\epsilon)^3}} e^{-\delta^2/\epsilon(1-\epsilon)}$
Meanders	$\frac{\delta}{\omega \sqrt{\pi \epsilon^3 (1-\epsilon)}} (1 - e^{-4\delta\omega/(1-\epsilon)}) e^{-(\epsilon\omega - \delta)^2/\epsilon(1-\epsilon)}$
Meanders (free endpoint)	$\frac{2\delta}{\sqrt{\epsilon^3}} e^{-\delta^2/\epsilon} \operatorname{erf}(\delta/\sqrt{1-\epsilon})$
Dyck paths (adsorbed phase)	via equation (51)
Dyck paths (special point)	$\frac{2}{\sqrt{\pi\epsilon(1-\epsilon)}} e^{-\delta^2/\epsilon(1-\epsilon)}$

In the desorbed phases these models have distributions peaking away from the hard wall, consistent with grafted directed polymers tending to drift away from the hard wall forming areas of lower density close to the hard wall, and higher density further away. This is seen in figure 5 for Dyck paths, and also in figures 7 and 8, for models of meanders. In the context of figure 1, this shows that particles close to the hard wall has to overcome entropic repulsion to migrate away from the hard wall, and this is the mechanism underlying the absorption and stabilisation of molecules by a system of linear polymers grafted to a hard wall, for example in drug eluding stents or nanoparticle-polymer systems. Observe that in the adsorbed phase the polymer is fully adsorbed, and this mechanism is not operative. This is also the case at the special point, where the probability density decreases monotonically with distance from the hard wall.

Appendix A

In this appendix we give a summary of the derivation of equations (18) and (19).

The asymptotic approximation of the factorial can be determined using a symbolic computations program [20]:

$$n! = \sqrt{2\pi n} n^n e^{-n} \left(1 + \frac{1}{12n} + \frac{\xi}{n^2}\right), \quad \text{where } \xi = c_0 + o(1). \quad (64)$$

Here, ξ is a function of n and it may be verified that $\xi = c_0 + O(1/n)$ where c_0 is a non-zero constant.

Noting that $\sqrt{1 + 1/6n} = 1 + 1/12n + O(1/n^2)$, this may be written in the form

$$n! = \sqrt{\pi(2n + 1/3)} n^n e^{-n} \left(1 + \frac{\zeta}{n^2}\right), \quad \text{where } \zeta = c_1 + o(1) \quad (65)$$

where c_1 is again a non-zero constant and $\zeta = c_1 + O(1/n)$. This gives equation (10).

Next, consider the left hand side of equation (18). This is of the generic form

$$A = \binom{2\lfloor \lambda n \rfloor}{\lfloor \lambda n \rfloor + \lfloor \delta \sqrt{n} \rfloor + \lfloor \kappa \sqrt{n} \rfloor + c} = \frac{(2\lfloor \lambda n \rfloor)!}{(\lfloor \lambda n \rfloor + \lfloor \delta \sqrt{n} \rfloor + \lfloor \kappa \sqrt{n} \rfloor + c)! (\lfloor \lambda n \rfloor - \lfloor \delta \sqrt{n} \rfloor - \lfloor \kappa \sqrt{n} \rfloor - c)!}$$

To obtain equation (18) put $c = 0$ and change the sign of $\lfloor \kappa \sqrt{n} \rfloor$, and for equation (19) put $c = 1$.

Approximate the factorials using equation (65). Making the following substitutions

$$\begin{aligned} a_1 &= \pi(4\lambda n + 1/3), \\ a_2 &= (\delta + \kappa)\sqrt{n} + \lambda n + c, \\ a_3 &= -(\delta + \kappa)\sqrt{n} - \lambda n - c, \\ a_4 &= \pi(2(\delta + \kappa)\sqrt{n} + 2\lambda n + 2c + 1/3), \\ a_5 &= -(\delta + \kappa)\sqrt{n} + \lambda n - c, \\ a_6 &= (\delta + \kappa)\sqrt{n} - \lambda n + c, \\ a_7 &= \pi(-2(\delta + \kappa)\sqrt{n} + 2\lambda n - 2c + 1/3), \\ a_8 &= 2\lambda n, \end{aligned}$$

gives

$$A = \frac{\sqrt{a_1} a_8^{a_8} e^{-2\lambda n} (1 + \zeta/(4\lambda^2 n^2))}{\sqrt{a_4} a_2^{a_2} e^{a_3} (1 + \zeta/a_2^2) \sqrt{a_7} a_5^{a_5} e^{a_6} (1 + \zeta/a_5^2)} \quad (66)$$

Take the logarithm of A , and expand asymptotically in n . The terms depending on ζ give the error, and this is, asymptotically in n ,

$$e^{\text{Error}} = \frac{(1 + \zeta/(4\lambda^2 n^2))}{(1 + \zeta/a_2^2)(1 + \zeta/a_5^2)} = 1 - \frac{7\zeta}{4\lambda^2 n^2} - \frac{6\zeta(\delta + \kappa)^2}{\lambda^4 n^3} + O(\lambda^{-4} n^{-7/2}). \quad (67)$$

This approaches 1 as $n \rightarrow \infty$ for any fixed $\lambda > 0$. Taking the logarithm of A and expanding asymptotically in n gives the result

$$\begin{aligned} \log A &= \lambda n \log 4 - (\log \pi)/2 - 2\delta\kappa/\lambda - \kappa^2/\lambda - (\log \lambda)/2 - \delta^2/\lambda \\ &\quad - (\log n)/2 - 2(\delta + \kappa)c/(\lambda\sqrt{n}) + (4\delta^2 + 8\delta\kappa + 4\kappa^2 - \lambda)/(8\lambda^2 n) \\ &\quad + (\delta + \kappa)c/(\lambda^2 n^{3/2}) + \text{Error} \end{aligned}$$

Exponentiating and simplifying then produces

$$A = \frac{e^{-(8\lambda(\delta + \kappa)^2 n^{3/2} + 16c\lambda(\delta + \kappa)n - (4(\delta + \kappa)^2 - \lambda)\sqrt{n} - 8c(\delta + \kappa))}/(8\lambda^2 n^{3/2}) e^{\text{Error}}}{\sqrt{\pi\lambda n}} 4^{\lambda n}. \quad (68)$$

In the event that δ or κ becomes large, the Error can similarly be expanded asymptotically in $\delta + \kappa = \ell$ to see that

$$e^{\text{Error}} = 1 + \frac{\zeta}{4\lambda^2 n^2} - \frac{\zeta(4\lambda^2 n^2 + \zeta)}{(\delta + \kappa)^2 \lambda^2 n^3} + \frac{\zeta c(4\lambda^2 n^2 + \zeta)}{(\delta + \kappa)^3 \lambda^2 n^{7/2}} + O((\delta + \kappa)^{-4}). \quad (69)$$

Thus, it follows that, for any fixed $\lambda > 0$,

$$A = \frac{e^{-(8\lambda(\delta+\kappa)^2n^{3/2}+16c\lambda(\delta+\kappa)n-(4(\delta+\kappa)^2-\lambda)\sqrt{n}-8c(\delta+\kappa))/(8\lambda^2n^{3/2})}}{\sqrt{\pi\lambda n}} 4^{\lambda n} \times \left(1 + \frac{\zeta}{4\lambda^2n^2} - \frac{\zeta(4\lambda^2n^2+\zeta)}{(\delta+\kappa)^2\lambda^2n^3} + O((\delta+\kappa)^{-3}n^{-3/2})\right). \quad (70)$$

Notice that since ζ is not a function of (δ, κ) and approaches a constant as $n \rightarrow \infty$, there is a uniform bound on the Error for any fixed $\kappa > 0$ and $\lambda > 0$ when $n \geq N_0 > 0$ and for all $\delta \geq \delta_0 > 0$ (where δ_0 is a fixed constant). In the limit $n \rightarrow \infty$ the Error approaches 0.

Putting $c = 1$, $\lambda = \sigma$, $\delta = \omega$ and $\kappa = \delta$ gives equation (19) after simplification. Putting $c = 0$ instead, and $\lambda = \sigma$, $\delta = \omega$ and $\kappa = -\delta$ gives equation (18) after simplification.

Acknowledgements: EJJvR acknowledges financial support from NSERC (Canada) in the form of Discovery Grant RGPIN-2019-06303.

References

- [1] GB Arfken and H-J Weber. Mathematical methods for physicists. Academic Press, Orlando, FL, 1967.
- [2] MT Batchelor and CM Yung. Exact results for the adsorption of a flexible self-avoiding polymer chain in two dimensions. Phys Rev Lett, 74:2026–2029, 1995.
- [3] R Brak, JW Essam, and AL Owczarek. New results for directed vesicles and chains near an attractive wall. J Stat Phys, 93:155–192, 1998.
- [4] R Brak, JW Essam, and AL Owczarek. Partial difference equation method for lattice path problems. Ann Comb, 3:265–275, 1999.
- [5] R Brak, AJ Guttmann, and SG Whittington. A collapse transition in a directed walk model. J Math Chem, 8:255–267, 1991.
- [6] R Brak, AJ Guttmann, and SG Whittington. A collapse transition in a directed walk model. J Phys A: Math Gen, 25:2437–2446, 1992.
- [7] R Brak, AL Owczarek, A Rechnitzer, and SG Whittington. A directed walk model of a long chain polymer in a slit with attractive walls. J Phys A: Math Gen, 38:4309–4325, 2005.
- [8] MCTP Carvalho and V Privman. Directed walk models of polymers at interfaces. J Phys A: Math Gen, 21:L1033–L1037, 1988.
- [9] A Farb, PF Heller, S Shroff, L Cheng, FD Kolodgie, AJ Carter, DS Scott, J Froehlich, and R Virmani. Pathological analysis of local delivery of paclitaxel via a polymer-coated stent. Circulation, 104(4):473–479, 2001.
- [10] Gerard Fleer, MA Cohen Stuart, Jan MHM Scheutjens, T Cosgrove, and B Vincent. Polymers at interfaces. Springer Science & Business Media, 1993.
- [11] G Forgacs. Unbinding of semiflexible directed polymers in 1+1 dimensions. J Phys A: Math Gen, 24(18):L1099–L1103, 1991.
- [12] DP Foster. Exact evaluation of the collapse phase boundary for two-dimensional directed polymers. J Phys A: Math Gen, 23:L1135–L1138, 1990.

- [13] GK Iliev and EJ Janse van Rensburg. Directed path models of adsorbing and pulled copolymers. *J Stat Mech: Theo Expr*, 2012:P01019, 2012.
- [14] EJ Janse van Rensburg. Square lattice directed paths adsorbing on the line $y = qx$. *J Stat Mech: Theo Expr*, 2005:P09010, 2005.
- [15] EJ Janse van Rensburg. The adsorption transition in directed paths. *J Stat Mech: Theo Expr*, 2010:P08030, 2010.
- [16] EJ Janse van Rensburg. The statistical mechanics of interacting walks, polygons, animals and vesicles, 2nd ed. Oxford Lecture Series in Mathematics and its Applications. Oxford University Press, 2015.
- [17] EJ Janse van Rensburg and T Prellberg. The pressure exerted by adsorbing directed lattice paths and staircase polygons. *J Phys A: Math Gen*, 46:115202, 2013.
- [18] N Jawahar and SN Meyyanathan. Polymeric nanoparticles for drug delivery and targeting: A comprehensive review. *Int J Health & Allied Sci*, 1(4):217, 2012.
- [19] WB Liechty, DR Kryscio, BV Slaughter, and NA Peppas. Polymers for drug delivery systems. *Ann Rev Chem Biomol Eng*, 1:149, 2010.
- [20] a division of Waterloo Maple Inc. Maplesoft. Maple. A division of Waterloo Maple Inc. (Waterloo Ontario), 2017.
- [21] DH Napper. Polymeric stabilization of colloidal dispersions, volume 3. Academic Press, 1983.
- [22] V Privman, G Forgacs, and HL Frisch. New solvable model of polymer-chain adsorption at a surface. *Phys Rev B*, 37:9897–9900, 1988.
- [23] A Rechnitzer and EJ Janse van Rensburg. Exchange relations, Dyck paths and copolymer adsorption. *Disc Appl Math*, 140:49–71, 2004.
- [24] Dirk Schmaljohann. Thermo- and ph-responsive polymers in drug delivery. *Advanced drug delivery reviews*, 58(15):1655–1670, 2006.
- [25] A Srivastava, T Yadav, S Sharma, A Nayak, AA Kumari, and N Mishra. Polymers in drug delivery. *J Biosci Med*, 4(1):69–84, 2015.
- [26] H Terayama, K Okumura, K Sakai, K Torigoe, and K Esumi. Aqueous dispersion behavior of drug particles by addition of surfactant and polymer. *Colloids and Surfaces B: Biointerfaces*, 20(1):73–77, 2001.
- [27] I Vardi. Computational Recreations in Mathematics. Addison-Wesley, 1991.
- [28] SG Whittington. A directed-walk model of copolymer adsorption. *J Phys A: Math Gen*, 31:8797–8803, 1998.